On the broadening of the magnetic entropy change due to Curie temperature distribution

Pablo Alvarez-Alonso, José L. Sánchez Llamazares, César F. Sánchez-Valdés, Gabriel J. Cuello, Victorino Franco, Pedro Gorria, and Jesús A. Blanco

Articles you may be interested in

Magnetocaloric effect from indirect measurements: Magnetization and heat capacity
Journal of Applied Physics **86**, 565 (1999); 10.1063/1.370767

Field dependence of the magnetocaloric effect in materials with a second order phase transition: A master curve for the magnetic entropy change
Applied Physics Letters **89**, 222512 (2006); 10.1063/1.2399361

Enhanced refrigerant capacity in two-phase nanocrystalline/amorphous $NdPrFe_{17}$ melt-spun ribbons
Applied Physics Letters **104**, 212401 (2014); 10.1063/1.4879544

Influence of the demagnetizing factor on the magnetocaloric effect: Critical scaling and numerical simulations
Applied Physics Letters **104**, 252405 (2014); 10.1063/1.4885110

Magnetic field dependence of magnetic entropy change in nanocrystalline and polycrystalline manganites $La_{1-x}M_xMnO_3 \, (M = Ca, Sr)$
Journal of Applied Physics **108**, 113913 (2010); 10.1063/1.3517831

Influence of the demagnetizing field on the determination of the magnetocaloric effect from magnetization curves
Journal of Applied Physics **105**, 07A919 (2009); 10.1063/1.3067463

On the broadening of the magnetic entropy change due to Curie temperature distribution

Pablo Alvarez-Alonso,[1] José L. Sánchez Llamazares,[2] César F. Sánchez-Valdés,[2] Gabriel J. Cuello,[3] Victorino Franco,[4] Pedro Gorria,[5,a)] and Jesús A. Blanco[6]

[1]*Dept. Electricidad y Electrónica, Universidad del País Vasco, Barrio Sarriena s/n, 48940 Leioa, Spain*
[2]*División de Materiales Avanzados, IPCyT, Camino a la presa San José 2055, 78216, San Luis Potosí, Mexico*
[3]*Institute Laue Langevin, 6 rue Jules Horowitz, 38042 Grenoble, France*
[4]*Dept. Física de la Materia Condensada, ICMSE-CSIC, Univ. Sevilla, P.O. Box 1065, 41080 Sevilla, Spain*
[5]*Departamento de Física, EPI, Universidad de Oviedo, 33203 Gijón, Spain*
[6]*Departamento de Física, Universidad de Oviedo, Calvo Sotelo s/n, 33007 Oviedo, Spain*

We have studied the correlation between the broadening of the isothermal magnetic entropy change and the Curie temperature (T_C) distribution in nanostructured Pr_2Fe_{17} and Nd_2Fe_{17} alloys produced by high-energy ball-milling after milling times of 10, 20, and 40 h. The changes in the microstructure affect the Fe local environments and as a consequence the magnetic interactions, giving rise to T_C distributions centered around 285 K and 330 K for the Pr_2Fe_{17} and Nd_2Fe_{17} alloys, respectively. The width of the distributions enlarges (up to 60 K) as the milling-time increases, and consequently, the isothermal magnetic entropy change curves show an extended full width at half maximum. © *2014 AIP Publishing LLC*. [http://dx.doi.org/10.1063/1.4867346]

Magnetic refrigeration, the main application of the magneto-caloric (MC) effect, is potentially called to replace conventional vapor-cycle technology due to its higher energy efficiency and because it avoids green-house effect and depletion of ozone.[1–3] Therefore, it is necessary to develop materials with large MC effect in broad temperature intervals around room temperature.

The MC materials usually exhibit useful working temperature intervals of about 20 K,[4] under magnetic field changes of 2 T, but often a refrigeration system demands a working temperature range that could reach 50 K or more. Thus, the increase of the temperature range without reducing their refrigerant capacity is a crucial aspect that MC materials must fulfill if their utilization in magnetic refrigeration technology is pursued. One of the material processing methods already used to enlarge the temperature range in which the maximum isothermal magnetic entropy change takes place is the mechanical milling of the MC material.[5–7] In fact, the nanocrystallization of ferromagnetic R_2Fe_{17} compounds (R = Pr and Nd) by means of ball milling has been proved as an illustrative example of this method, which leads to the enhancement of the refrigerant temperature range and the refrigerant capacity.[8,9]

Moreover, the Curie temperature (T_C) is strongly affected by the modification of the Fe–Fe interatomic distances in a number of Fe-based alloys exhibiting magneto-volume anomalies.[10] Changes in the material microstructure can produce local inhomogeneities around the Fe atoms, and a distribution of Fe-Fe interatomic distances affecting the exchange interactions. The latter would affect the value of the T_C in the sense that instead of a unique value for the T_C a more reliable picture is to consider also a distribution function for this magnitude in the mechanically treated material. This distribution of T_C values can induce a broadening of the magnetic entropy change curves. In this paper, we report on the broadening of the isothermal magnetic entropy change and the Curie temperature distribution in ball-milled Pr_2Fe_{17} and Nd_2Fe_{17} compounds.

As-cast pellets and 10, 20, and 40 h ball-milled samples were fabricated following the procedure described elsewhere.[11] Scanning (SEM) and transmission (TEM) electron microscopy were used to study the microstructure and morphology of the milled powders. Room temperature x-ray powder diffraction patterns were collected in a high-resolution x-ray powder diffractometer (Seifert model XRD3000) using graphite-monochromated Cu Kα radiation ($\lambda = 1.5418$ Å). Room temperature neutron powder diffraction patterns were collected on the D1B two-axis neutron diffractometer (ILL, Grenoble, France) using a neutron wavelength of 2.52 Å. Le Bail analyses were performed using the FullProf suite package.[12]

Magnetization vs. temperature curves under a constant applied magnetic field of $\mu_o H = 20$ mT in the temperature range 250–400 K were obtained in a Faraday balance. Isothermal $M(\mu_o H)$ curves were measured in two magnetometers, a Lakeshore VSM 7407 (85–420 K) and in a Quantum Design PPMS (200–400 K). The isothermal magnetic entropy change, ΔS_M, was determined through the appropriate Maxwell relation.[13]

SEM images reveal that the Pr_2Fe_{17} and Nd_2Fe_{17} milled powders are agglomerations of micronic grains (0.5–10 μm) with rounded borders and narrower size distribution as the milling-time is increased.[8,9] Higher magnification images obtained by TEM show grains formed by crystallites of nanometric size; the histograms describing the crystallite size distribution for the BM-10h and BM-20h compounds (powders ball-milled for 10 and 20 h, respectively) follow log-normal functions with average size of the crystallites below 25 nm (see Table I). For the BM-40h samples, not enough crystallites

TABLE I. Structural and magnetic data (the crystallographic parameters were obtained from the x-ray and neutron powder diffraction patterns).

	Pr_2Fe_{17}				Nd_2Fe_{17}			
	Bulk	BM-10h	BM-20h	BM-40h	Bulk	BM-10h	BM-20h	BM-40h
a(Å)	8.584(1)	8.580(1)	8. 582(1)	8.583(1)	8.582(1)	8.580(1)	8.578(1)	8.578(1)
b(Å)	12.460(1)	12.455(1)	12. 458(1)	12.453(1)	12.459(1)	12.455(1)	12.453(1)	12.454(1)
τ_{TEM} (nm)	...	23(1)	18(1)	*	...	17(3)	10(2)	...
τ_{Diff} (nm)	...	20(1)	17(1)	11(1)	...	18(1)	15(1)	11(1)
$\bar{T}_C$(K)	286(2)	290(5)	290(10)	290(10)	339(2)	340(10)	340(10)	340(10)

appeared in the TEM images to obtain reliable statistical information. The upper right inset in Fig. 1 shows a representative TEM image of Nd_2Fe_{17} BM-40h powders.

In Fig. 1, the room temperature neutron powder diffraction patterns corresponding to the Nd_2Fe_{17} samples are depicted. All the intensity peaks observed in the pattern of the starting bulk alloy correspond to Bragg reflections belonging to a Nd_2Fe_{17} phase with the rhombohedral Th_2Zn_{17}-type crystal structure; the estimated lattice parameters (see Table I) agree with those previously reported.[14] The ball-milling process maintains the Th_2Zn_{17}-type crystal structure with almost unchanged values of the cell parameters, but alters the microstructure (see Table I). Details of the followed procedure are described elsewhere.[15]

Figure 2 shows the magnetization as a function of the temperature, $M(T)$ curves. Those curves were composed with the points corresponding to $\mu_o H = 1\,T$ of the isothermal $M(\mu_o H)$ measurements. Notice how the shape of the $M(T)$ curves changes as the milling-time increases: the ferro-to-paramagnetic phase transition becomes poorly defined. However, the position of the dM/dT vs. T curve minima (see insets in Figure 2) remains almost unaltered (see Table I). The latter can be attributed to the effect of a change in the local environment of Fe atoms at the grain boundaries, which
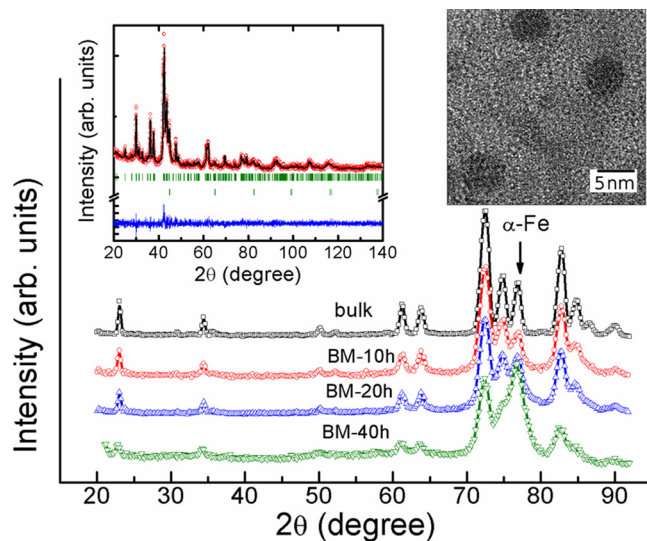
modifies the magnetic interactions[16] and, thus, the Curie temperature of certain regions. Hence, we could picture the nanostructured powders having a distribution of Fe-Fe interatomic distances around the value for the Bulk alloys giving rise to a distribution of Curie temperature values.[8,9] Then, we describe the temperature dependence of the magnetization $M(T)$ by a superposition of individual power-law functions, according to[17]

$$M(T) = m_0 \int_{T_C} \left(\frac{T_C - T}{T_C}\right)^{\beta} \theta(T_C - T)\rho(T_C, \alpha)dT_C. \quad (1)$$

Here, m_0 is a factor proportional to the saturation magnetization, β is the temperature critical exponent of the magnetization, $\theta(x)$ is the Heavyside function (that ensures vanishing magnetization values at $T = T_C$), and $\rho(T_C, \alpha)$ a sample-specific T_C distribution function with parameters set α. For the present case, we have assumed a Gaussian distribution

$$\rho\left(T_C, \overline{T_C}, \Delta T_C\right) = \frac{1}{\sqrt{2\pi}\Delta T_C}\exp\left(-\frac{1}{2}\frac{\left(T_C - \overline{T_C}\right)}{\Delta T_C^2}\right) \quad (2)$$

FIG. 1. Room temperature neutron powder diffraction patterns corresponding to bulk, BM-10h, BM-20h, and BM-40h Nd_2Fe_{17} alloys. *Upper left inset*: Le Bail fit of the x-ray powder diffraction pattern collected for BM-20h Pr_2Fe_{17} sample. *Upper right inset*: TEM image of the BM-40h Nd_2Fe_{17} sample.
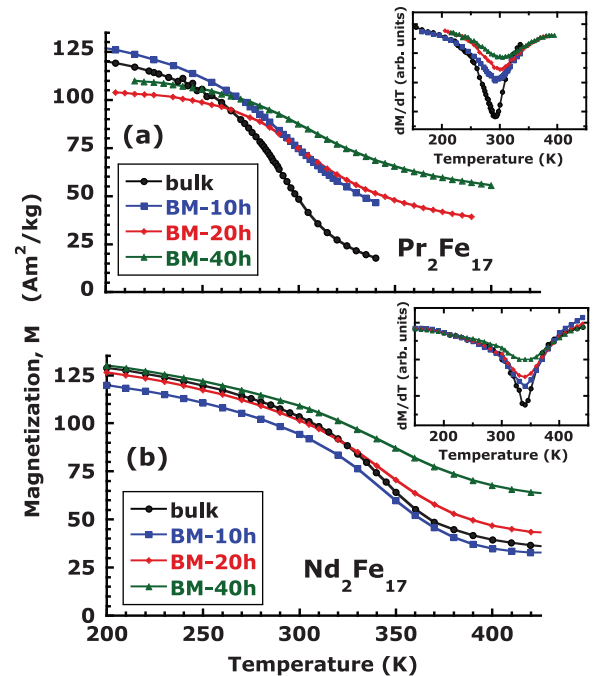

FIG. 2. Temperature dependence of the magnetization under an applied magnetic field of $1\,T$ for the bulk and BM samples, (a) Pr_2Fe_{17} and (b) Nd_2Fe_{17}. The two insets show the temperature derivatives of the magnetization.
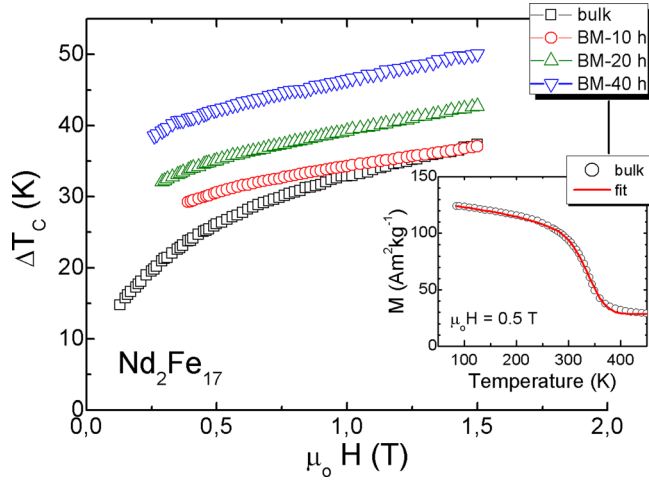
FIG. 3. Magnetic field dependence of the ΔT_C for bulk and BM Nd_2Fe_{17} samples. Inset: temperature dependence of the magnetization for the bulk Nd_2Fe_{17} alloy (see text for details).

FIG. 4. Temperature dependence of the magnetic entropy change under $\mu_o\Delta H = 1.5$ T for the bulk and BM Pr_2Fe_{17} and Nd_2Fe_{17} samples.

being $\bar{T}_C$ and ΔT_C the average value and width of the T_C distribution.

Although the value of T_C is unique for any ferromagnetic single-phase alloy and this value must be determined under zero applied magnetic field, if the minimum of the dM/dT vs. T curves is chosen as the value for the T_C of the material, such minimum of the dM/d$T(T)$ curve exhibits a broadening as the applied magnetic field is increased. The inset in Fig. 3 shows the fit obtained for the temperature dependence of the magnetization in bulk Nd_2Fe_{17} alloy for $\mu_oH = 0.5$ T following this approach. The T_C distribution width (see Figure 3) augments with milling-time for each magnetic field. The magnetic field dependence of the width follows a power law, $\Delta T_C(H) = \Delta T_C^0 + cH^{1/\eta}$, with η related with the critical exponents of the transition, as Berger *et al.* have shown.[17] The fit to a power law gives for Nd_2Fe_{17}: $\eta^{Bulk} = 1.9 \pm 0.2$, $\eta^{BM-10h} = 3.0 \pm 0.3$, $\eta^{BM-20h} = 2.4 \pm 0.2$, and $\eta^{BM-40h} = 2.8 \pm 0.3$. The differences in these values indicate variations in the magnetic interactions of the alloys and how they are affected by the applied magnetic field.

Fig. 4 plots the temperature dependence of the magnetic entropy change at $\mu_oH = 1.5$ T, for the studied samples. The temperatures at which the curves reach their maximum are similar for the four samples ($\sim T_C$). However, for the milled samples the maximum values of $|\Delta S_M|$ diminish with the milling-time because the drop of the magnetization is less pronounced as milling-time increases.

In summary, ball-milled Pr_2Fe_{17} and Nd_2Fe_{17} alloys maintain the Th_2Zn_{17}-type crystal structure but their crystallite size is reduced below 25 nm. The local environment of Fe atoms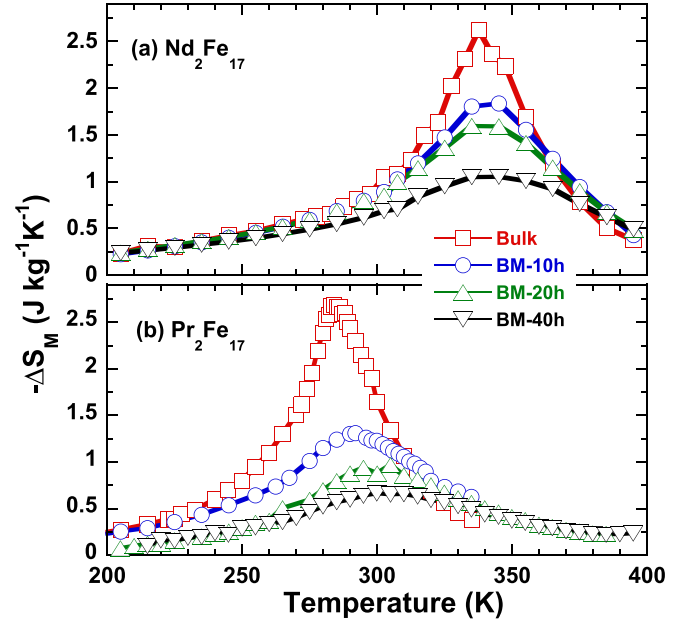 seems to be altered during the nanocrystallization process, giving rise to a Curie temperature distribution around the bulk's value. Fitting the magnetization vs. temperature curves with a Gaussian-type Curie temperature distribution, we found that the longer milling, the wider the T_C distribution, which correlates to the enlargement of the magnetic entropy change full width at half maximum.

[1] V. K. Pecharsky and J. Gschneidner, Int. J. Refrig. **29**, 1239 (2006).
[2] A. Tishin, J. Magn. Magn. Mater. **316**, 351 (2007).
[3] V. Franco *et al.*, Annu. Rev. Mater. Res. **42**, 305 (2012).
[4] K. Gschneidner *et al.*, Scr. Mater. **67**, 572 (2012).
[5] B. Chevalier *et al.*, Appl. Phys. A **80**, 601 (2005).
[6] P. Gorria *et al.*, J. Phys. D: Appl. Phys. **41**, 192003 (2008).
[7] J. Gass *et al.*, J. Appl. Phys. **103**, 07B309 (2008).
[8] P. Gorria *et al.*, Acta Mater. **57**, 1724 (2009).
[9] P. Álvarez *et al.*, J. Phys.: Condens. Matter **22**, 216005 (2010).
[10] P. Álvarez-Alonso *et al.*, Phys. Rev. B **86**, 184411 (2012).
[11] P. Alvarez *et al.*, J. Non-Cryst. Solids **354**, 5172 (2008).
[12] J. Rodríguez-Carvajal, Physica B **192**, 55 (1993).
[13] P. Álvarez *et al.*, J. Alloys Compd. **504**, S150 (2010).
[14] G. Long *et al.*, J. Appl. Phys. **76**, 5383 (1994).
[15] D. Martinez-Blanco *et al.*, J. Phys.: Condens. Matter **20**, 335213 (2008).
[16] G. Campillo *et al.*, J. Magn. Magn. Mater. **237**, 61 (2001).
[17] A. Berger *et al.*, J. Appl. Phys. **91**, 8393 (2002).